Thermodynamically Consistent Modeling of a Liquid-Phase Nonisothermal Packed-Bed Reactor

Faisal H. Syed and Ravindra Datta
Dept. of Chemical Engineering, Worcester Polytechnic Institute, Worcester, MA 01609

Kyle L. Jensen
Bandag, Inc., 2905 N. Highway 61, Muscatine, IA 52761

The equilibrium-limited steady-state nonisothermal behavior of an integral packed-bed reactor is described for the liquid-phase synthesis of ethyl tert-butyl ether with a model that is inherently consistent with thermodynamics. It involves a coupled one-dimensional mass- and enthalpy-balance equation with temperature-dependent thermochemical properties and reaction equilibria. The model accounts for the nonideal nature of the liquid-phase reaction system by utilizing species activities in the rate expression for the reversible reaction, which is also consistent with thermodynamic equilibrium. Experiments agreed well with theory with all of the kinetic, thermodynamic and other physicochemical parameters being obtained from independent experiments, indicating that the theoretical approach is robust. Further, the results clearly endorse the use of species activities rather than concentration, or mole fractions, in the rate expression for the nonideal liquid-phase reactions. There is a paucity of such studies in the literature, especially for liquid-phase nonisothermal packed-bed reactor analysis.

Introduction

A variety of mathematical models exist in the literature for analyzing the behavior of nonisothermal packed-bed reactors, ranging in complexity from one-dimensional pseudohomogeneous to two-dimensional heterogeneous models (Aris, 1969; Holland and Anthony, 1979; Denbigh and Turner, 1984; Lee, 1985; Froment and Bischoff, 1990). Although the two-dimensional heterogeneous model is the most detailed, the computational effort in solving the resulting mass and energy equations is substantial. Therefore, the one-dimensional models are frequently preferred (Froment and Bischoff, 1990). However, the existing one-dimensional models have certain deficiencies, particularly for nonideal liquid-phase systems involving reversible reactions. In fact, there are internal inconsistencies in virtually all models for reversible reactions. For instance, while it is the norm to use temperature-dependent heat capacities and other thermodynamic properties in the thermodynamic equilibrium analysis, these terms are invariably assumed to be constant in the reactor enthalpy balance equations. Furthermore, reaction rate expressions are written almost invariably in terms of concentration, which is inconsistent with thermodynamic equilibrium where activities are utilized, especially for liquid-phase systems. Generally, there are also inconsistencies in the form of temperature dependence for equilibrium constants and that for the forward and reverse rate constants.

Due to a lack of satisfactory models for nonideal liquid-phase systems, a one-dimensional nonisothermal packed-bed reactor model for liquid-phase reversible reactions, which incorporates thermodynamic, kinetic, heat, and mass-transfer terms in a consistent manner, is utilized here for ethyl *tert*-butyl ether (ETBE) synthesis. ETBE is the ethanol counterpart of the more commonly used oxygenate methyl *tert*-butyl ether (MTBE). Recently, the use of MTBE has come under question from a variety of environmental groups. Although MTBE is effective in reducing carbon monoxide emissions and increasing gasoline octane levels, MTBE's high chemical stability and solubility in water (4.8 g/100 g water) threatens

Correspondence concerning this article should be addressed to R. Datta.

groundwater from leaking tanks. California, which represents about 25% of the world's annual MTBE market, has already passed legislation for its phase out, and is considering alternative additives like ETBE, *tert*-butanol, and *tert*-amyl methyl ether (Morse, 1999). Not only does ETBE provide similar, and in some cases, better gasoline blending properties than MTBE, it has the added advantage of being partly renewable. Furthermore, the water solubility of ETBE is only a quarter that of MTBE, which is a substantial advantage. Jensen and Datta (1995) and Jensen (1996) discuss in detail the reaction kinetics, equilibrium thermodynamics, and industrial packed-bed reactor schemes associated with ETBE production. The kinetics for this nonideal reaction system is modeled utilizing species activities, rather than the more typical concentration, or mole fraction. All other physicochemical parameters utilized in the reactor model were determined independently. The model is simple enough to be computationally convenient, but robust enough to provide accurate reactor behavior. The model is validated using experimental results, and further used to discuss reactor design issues for ETBE synthesis. The ability of the model to accurately predict the intensity and location of the hot spots enables the development of design strategies to reduce catalyst deactivation and enhance reactor performance.

Theory

Various one- and two-dimensional models exist for describing the fixed-bed reactor, that take into account axial mixing, intraparticle gradients, as well as radial variations (Lee, 1985; Tarhan, 1983). The model utilized here neglects axial dispersion and assumes the phenomenological model, $q_{rw} = U(T_a - T)$, for the radial heat flux at the wall based on an overall heat transfer coefficient U, a cross-sectional averaged bed temperature T, and a constant ambient temperature T_a. Further, the effectiveness factor η of the catalyst particles is assumed to be unity. These assumptions are later shown to be applicable for the case of ETBE synthesis. The adequacy of a one-dimensional model is supported by the results of Ferreira et al. (1996), which showed small differences, in most cases, between temperature profiles obtained using unidimensional and bidimensional models for MTBE synthesis.

Unlike typical packed-bed models, however, the species heat capacities, along with enthalpy and Gibbs free-energy change (or equilibrium constant) for the reaction, are allowed to vary with temperature within the reactor for consistency with thermodynamic reaction equilibria. The heat capacity of species j as a function of temperature is assumed to be of the standard form

$$C^o_{Pj} = a_j + b_j T + c_j T^2 + d_j T^3, \tag{1}$$

and the standard enthalpy change for the ith reaction,

$$\Delta H^o_{iT} \equiv \sum_{j=1}^{n} \nu_{ij} \Delta H^o_{fjT},$$

as a function of temperature, is obtained from the integrated form of the Kirchoff equation

$$\Delta H^o_{iT} = I_{iH} + \Delta a_i T + \frac{\Delta b_i}{2} T^2 + \frac{\Delta c_i}{3} T^3 + \frac{\Delta d_i}{4} T^4, \tag{2}$$

which when used in the v'ant Hoff equation provides the standard Gibbs free-energy change, or equivalently, the equilibrium constant, for reaction i

$$-\frac{\Delta G^o_{iT}}{RT} = \ln K_i = I_{iK} - \frac{I_{iH}}{RT} + \frac{\Delta a_i}{R} \ln T + \frac{\Delta b_i}{2R} T + \frac{\Delta c_i}{6R} T^2 + \frac{\Delta d_i}{12R} T^3. \tag{3}$$

In the preceding, the two constants of integration for reaction i, namely, I_{iH} and I_{iK}, are determined from Eqs. 2 and 3, respectively, by setting $T = T^o$, the standard temperature, along with the knowledge of the standard enthalpy and Gibbs free-energy change of reaction i, $\Delta H^o_{iT^o}$ and $\Delta G^o_{iT^o}$.

Defining conversion for our case of a single reaction ($q = 1$) for ETBE synthesis on the basis of the key limiting reactant, namely isobutylene (B), $X \equiv (F_B - F_{B0})/F_{B0}$, ethanol typically being 5% in excess of stoichiometric feed to suppress isobutylene dimerization, and using $dW = (1 - \epsilon_B)\rho_C \pi R_t^2 dz$, for a tubular reactor of radius R_t, results in the following cross-sectional area-averaged enthalpy and mass balances, respectively:

$$\frac{dT}{dz} = \pi R_t^2 (1 - \epsilon_B)\rho_C \left\{ \frac{(-\Delta H^o_{iT}) r_i + \dfrac{Ua(T_a - T)}{(1 - \epsilon_B)\rho_C}}{F_{B0}\left(\displaystyle\sum_{j=1}^{n} \Theta_j C^o_{Pj} + X \Delta C^o_{iP} \right)} \right\} \tag{4}$$

and

$$\frac{dX}{dz} = \pi R_t^2 (1 - \epsilon_B)\rho_C \left(\frac{-\nu_{iB}}{F_{B0}} \right) r_i, \tag{5}$$

which need to be simultaneously solved to determine the T and X profiles within the reactor. The reaction rate in the preceding equations is written in terms of activities. Using the Langmuir-Hinshelwood-Hougen-Watson (LHHW) formalism, in which each of the elementary steps is treated according to the thermodynamic transition-state theory (Jensen, 1996),

$$r_A = k_{si} a_A^2 \frac{\left(a_B - \dfrac{a_C}{a_A K_i} \right)}{(1 + K_A a_A)^3}, \tag{6}$$

where $a_j = x_j \gamma_j$, and the activity coefficients are calculated using the UNIFAC method. The rate constant, k_{si}, in Eq. 6 is written in the conventional Arrhenius form, with the preexponential factor and effective activation energy having values of 7.418×10^{12} mol/h·g and 60.4×10^3 J/mol, respectively (Jensen, 1996). The rate expression is based on a mechanism involving a three-site surface reactions as the rate-determining step, and utilizing the most abundant surface-species assumption for ethanol. This assumption is supported by the

large adsorption equilibrium constant of ethanol as compared to other species and given by Kitchaiya (1995) as

$$K_A = 27 \exp\left[\frac{11{,}000}{R}\left(\frac{1}{T} - \frac{1}{303}\right)\right]. \qquad (7)$$

The heat-capacity coefficients for the species involved, along with other relevant thermochemical data, are provided in Jensen and Datta (1995).

Experimental

Apparatus

In order to reduce the heat losses from a laboratory-scale reactor with high surface-to-volume ratio as compared with industrial units, a packed-bed tubular reactor was constructed by machining a cylindrical block of PFA Teflon (obtained from McMaster-Carr). Details of the reactor construction along with its dimensions are given in Figure 1. A cylindrical cavity (1/2 in. diameter, 10.5 in. length) was bored into the center of the block, which served as the tubular reactor. Multiple holes (1/16 in. in diameter) were drilled in the radial direction, axially spaced 0.5 in. apart in a spiral configuration, to house the inlet/outlet ports as well as thermocouples (Omega Type K, 1/16 in. O.D.) to measure the temperature. A removable top, secured by screws and aluminum supports allowed for easy loading/unloading of the catalyst. The catalyst was held in place with glass-wool plugs.

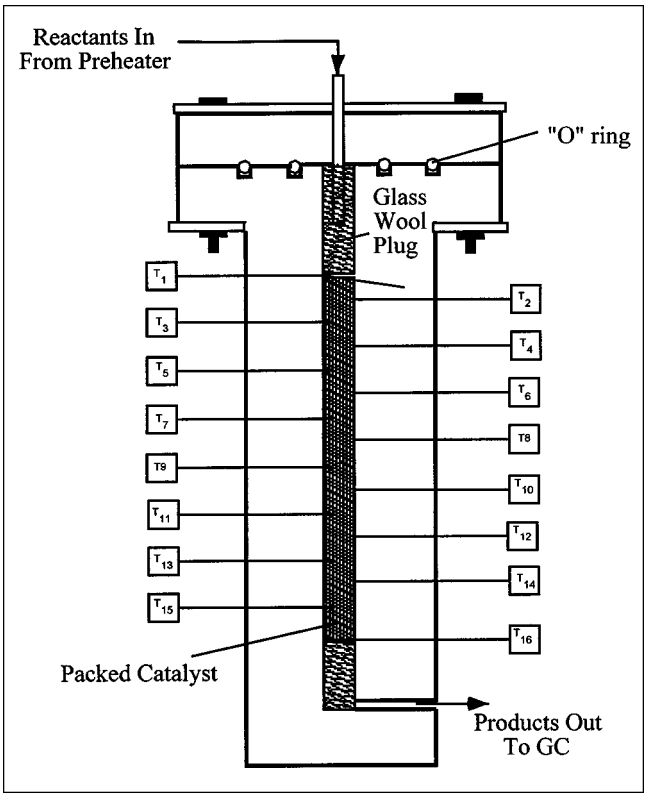

Figure 1. Design and dimensions of downward flow packed-bed Teflon reactor.

The desired amounts of ethanol, isobutylene, and any inert (*n*-heptane) were premixed in a stainless-steel cylinder, and then transferred to a 1000-mL syringe pump (Isco, Model 1000D). The syringe pump enabled the reactant to be fed in a steady pulse-free flow to the downflow reactor. The reactants were passed through a preheater and heated to the desired temperature before entering the unheated reactor. The system pressure was kept above the bubble point in the range of 200 to 250 psig using a back-pressure regulator (Upchurch Scientific, P738) to ensure liquid-phase operation.

Materials

Amberlyst-15 ion-exchange resin catalyst (obtained from Sigma) was treated by washing the resin with ethanol, followed by 1.0 N HNO_3 and then with ethanol again to remove any excess free acid remaining on the resin beads. After drying for 12 h in an oven under vacuum at 105°C, the resin was stored in a dessicator until used. The intact catalyst beads with an average particle diameter of 0.74 mm were used. Other physical properties of Amberlyst-15 are provided in Kunin et al. (1962). Amberlyst-15 swells to varying degrees depending upon the nature of the solvent. Its swelling in the presence of ethanol is substantial, and therefore to ensure consistent packing and bed porosity, it was packed in the reactor in the swollen state. This was accomplished by washing the dried catalyst with ethanol prior to packing in the reactor. Approximately 13.75 g of dry catalyst was thus packed, occupying the reactor length of 9.5 in.

Dehydrated 200 proof ethanol was obtained from Pharmco. CP grade isobutylene was obtained from Matheson with a purity greater than 99%. *n*-Heptane was used as an inert diluent in some of the experiments and was obtained from Fisher Scientific with a purity of 98%. These chemicals were used without any further pretreatment.

Procedure

To reduce the time to reach steady state, the catalyst bed was preheated to a temperature of 40–50°C by pumping preheated *n*-heptane through the system using a positive displacement pump (Gilson Medical, Model 305) prior to the introduction of the reaction mixture. The reactor was not heated externally. Once the bed was thus preheated, the syringe pump was started at preset values, and the reaction mixture was preheated to the desired reactor inlet temperature. The temperature profile of the catalyst bed was monitored continuously as a function of time using an automated data-acquisition system. Once a steady temperature profile had been achieved, the product was analyzed via gas chromatography to determine the overall conversion. An on-line liquid sampling valve (Valco, Model CL4WE) and a Perkin Elmer AutoSystem gas chromatograph were utilized for this purpose. A Porapak R column (Supleco, 1/8 in. x 6 ft) along with a thermal conductivity detector (TCD) were used. The gas chromatograph oven was held at 170°C, with helium as the carrier gas at a flow rate of 30 mL/min. The TCD detector temperature was held at 190°C. Isobutylene conversion, X, was computed

$$X = 1 - \frac{\omega_{B,\text{outlet}}}{\omega_{B,\text{inlet}}}, \qquad (8)$$

where ω_B is the mass fraction of isobutylene. The side products (that is, *tert*-butyl alcohol (TBA), di-isobutene) formed were insignificant, always being less than 1%, and were therefore neglected in further calculations.

Results and Discussion

Physical and thermodynamic parameters

The activity coefficients were computed using the UNIFAC method, which has been shown by Izquierdo et al. (1992) and others to provide accurate values for the MTBE and ETBE reaction mixtures. The value for bed porosity, $\epsilon_B = 0.62$, and the overall heat-transfer coefficient, U, were experimentally determined independently. The appropriate value of U was determined by conducting heat-transfer experiments with various reactant feed-mixture compositions and with the reactor packed with completely deactivated catalyst. The catalyst was deactivated by neutralizing (ion-exchanging) the acid sites with sodium hydroxide. The feed was preheated to a temperature of 343 K and allowed to flow through the reactor. Outlet concentration was verified by gas chromatography to ensure the absence of any reaction. By experimentally measuring the resulting steady-state temperature profile within the packed-bed, and using Eq. 4 with $r_i = X = 0$, an average value of $U = 7.0$ J/h·cm^2·K was obtained.

The effect of temperature on the species heat capacities is shown in Figure 2a, while the effect of temperature on the enthalpy change and Gibbs free-energy change for the reaction is shown in Figure 2b. It is clear from these figures that these quantities are substantially temperature dependent in the temperature range of interest, and consequently it would be erroneous to treat them as constant, as is typically done in reactor modeling. While the exothermicity of the reaction increases as the temperature increases, the negative Gibbs free-energy change for the reaction declines substantially, causing the equilibrium constant to decrease with temperature. The maximum obtainable conversion in conventional reactors is the equilibrium conversion, X_e. As shown in Figure 2c, although the equilibrium conversion at 300 K is approaching 95%, at higher temperatures (about 370 K) the conversion drops to less than 80%. This plot thus provides an upper limit to the reactor outlet temperature for a desired conversion.

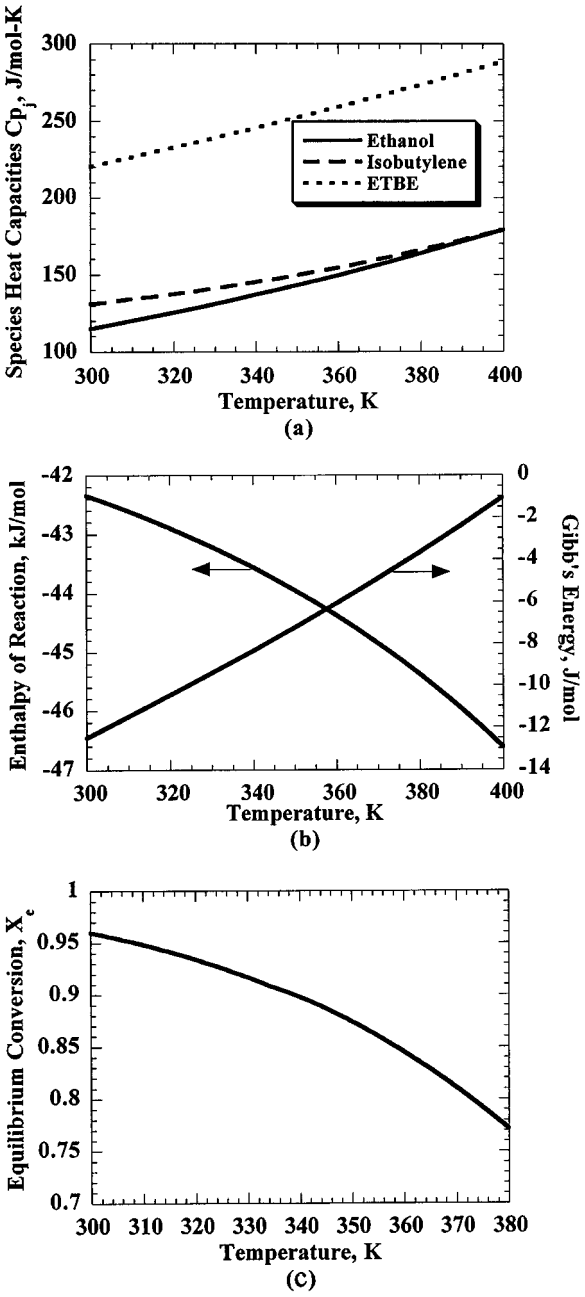

Figure 2. (a) Effect of temperature on species heat capacities; (b) enthalpy and Gibbs energy; (c) equilibrium conversion.

Reactor simulations

Equations 4 and 5 were simultaneously solved numerically using a modified fourth-order Runge-Kutta method, in which the species activities were updated using the UNIFAC method between each iteration. Typical temperature, conversion, and reaction-rate profiles for adiabatic and nonisothermal reactors as simulated by the theoretical model are shown in Figure 3 for a feed with an ethanol/isobutylene molar ratio, $\Theta_A = 1.05$, and a weight hourly space velocity (WHSV) of 5 h^{-1}. Further, $U = 0$ was used for simulating the adiabatic case, while the experimental value of $U = 7.0$ J/h·cm^2·K was used for the more realistic nonisothermal case. There is a sharp increase in the temperature (Figure 3a), the conversion (Figure 3b), as well as the rate of reaction (Figure 3c) in the inlet section of the reactor.

As the reactants enter the reactor, the reaction rate is slow due to the low feed temperature. As the reaction progresses, however, the heat generated by the reaction raises the temperature, thereby causing the reaction rate to increase sharply, resulting in even more heat being generated. However, since the rate constant of the reverse reaction increases even more rapidly with temperature than that of the forward reaction (that is, the thermodynamic equilibrium constant declines with temperature), and as the concentration of product increases within the reactor, the *net* rate of reaction, that is, the difference between forward and reverse rates, peaks sharply and then drops precipitously, approaching zero (Figure 3c), corresponding to thermodynamic equilibrium. There-

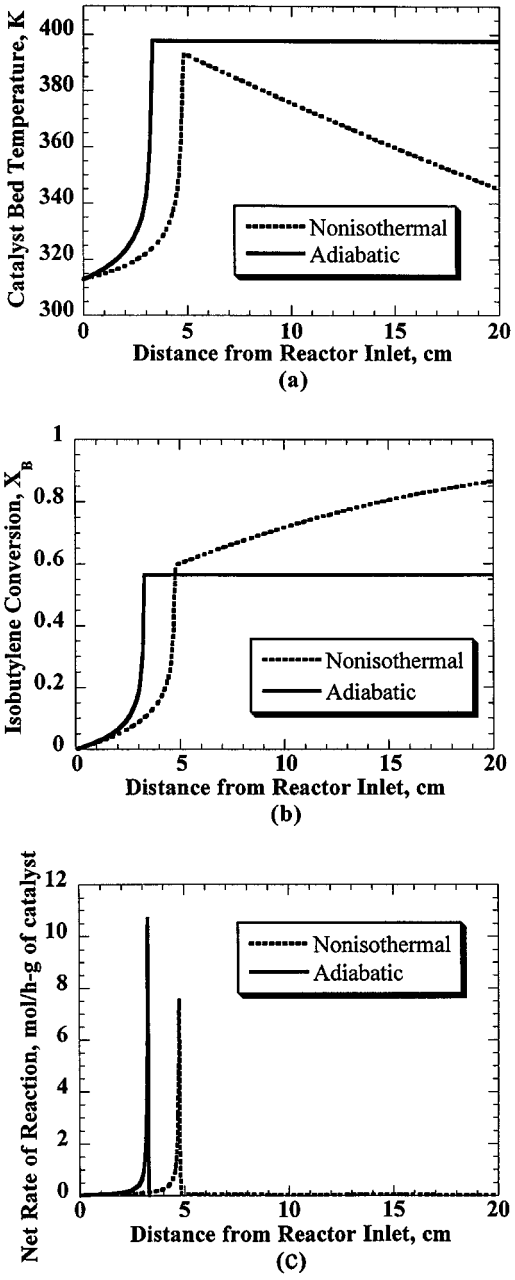

Figure 3. (a) Temperature, (b) conversion, and (c) net reaction rate profiles simulated for reactant feed containing no inert.

$\Theta_{EtOH} = 1.05$, WHSV = 5 h^{-1}, and $U = 0$ (adiabatic operations) and 7.0 J/h·cm^2·K (nonisothermal operation).

fore, the entrance region of the reactor can be deemed to be kinetically controlled. Further, since the rate of the reaction spikes within a narrow region of the catalyst bed close to the entrance, it is apparent that only a very small portion of the catalyst bed is actually responsible for the majority of the conversion (Figure 3b). If there is no heat loss from the reactor, that is, for strictly adiabatic operation, the temperature and the conversion remain constant thereafter. On the other hand, when there is a finite heat loss from the reactor walls, that is, for nonisothermal operation, the temperature drops gradually beyond the peak and the conversion concomitantly rises slowly, corresponding to the increase in the equilibrium constant with declining temperature. In other words, the conversion in this section of the reactor is thermodynamically controlled. It is noteworthy that the conversion for the nonisothermal case is substantially *higher* than that for the adiabatic case. Heat loss from the reactor also lowers the peak temperature and shifts it further downstream (Figure 3a).

Comparison of model and experiments

Experiments were first conducted in the absence of any inert component in the feed with the WHSV ranging from 4.4 h^{-1} to 32 h^{-1}, and an ethanol/isobutylene molar ratio, $\Theta_A = 1.05 \pm 0.02$. This slight stoichiometric excess of ethanol is maintained in industry to increase the isobutylene conversion and to prevent any side reactions such as isobutylene dimerization, which increases dramatically when ethanol mole fraction x_A in the reaction mixture is less than 0.05 (Brockwell, 1991). Otherwise, the large adsorption equilibrium constant of ethanol (Eq. 7) ensures that essentially all the catalyst sites are covered with ethanol and the probability of two adjacent adsorbed isobutylene molecules is quite low, thus effectively suppressing catalytic dimerization. The catalyst bed was preheated to a temperature of 313 K before reactant flow was commenced, as described earlier. The temperature profile of the reactor was continuously monitored until a steady-state operation was achieved, at which point two separate outlet composition measurements, taken 20 min apart, were taken to further ensure steady-state operation.

The resulting temperature profiles for WHSVs ranging from 4.4 h^{-1} to 32 h^{-1} are shown in Figure 4 along with model predictions, and are qualitatively similar to the temperature profiles obtained experimentally by Ladisch et al. (1993), for the case of MTBE synthesis in a pilot-scale integral packed-bed reactor. For the lower space velocity, WHSV = 4.4 h^{-1}, the temperature in the reactor rises dramatically from an inlet temperature of 313 K to a peak temperature of

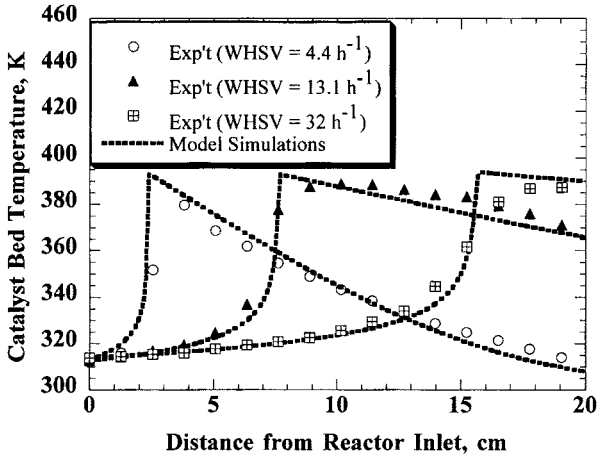

Figure 4. Experimental results vs. theoretical model for catalyst-bed temperature profile for feed containing no inert.

$\Theta_{EtOH} = 1.05$, WHSV ranging from 4.4 to 32 h^{-1}, inlet temperature of 313 K, and $U = 7.0$ J/h·cm^2·K.

around 380 K, within a relatively narrow region, that is, within 4 cm from the entrance of the catalyst bed. The temperature thereafter begins to decrease due to the heat loss from the reactor to a final exit temperature of around 310 K. Increasing the WHSV shifts the location of the temperature peak farther downstream, but the peak height (temperature) remains similar. Using $U = 7.0$ J/h·cm^2·K and other independently measured parameters as described earlier, it is seen that good agreement is obtained between the experiments and the predicted results. It may be remarked that peak location and intensity are highly parametrically sensitive, and the good agreement without any fitted parameters implies a robust model.

Axial dispersion and intraparticle diffusion

In the one-dimensional model described by Eqs. 4 and 5, axial dispersion is assumed to be negligible and the catalyst particle effectiveness factor is assumed to be unity. The good agreement between experiments and theory for the peak intensity and location appears to confirm the validity of the lack of substantial axial dispersion. Furthermore, it has been shown that the axial dispersion terms (that is, heat and mass) can be neglected for bed lengths greater than 150 times the catalyst particle diameter (Carberry, 1976; Lee, 1985).

The good agreement appears to also lend credence to the assumption of substantial absence of intraparticle heat and mass-transport limitations. Intraparticle diffusion has been shown to significantly limit the rate of reaction only at high temperatures, that is, in excess of 333 K, for the case of MTBE synthesis over Amberlyst-15 catalyst with particle diameter of 0.74 mm (Zhang and Datta, 1995), when alcohol is present in slight stoichiometric excess. If this is not the case, the rates of reaction can become very high in regions of alcohol depletion due to the inverse dependence of the rate on alcohol concentration (Jensen, 1996). Thus, alcohol depletion within the catalyst particle can cause the effectiveness factor to exceed unity even at low temperatures (Rehfinger and Hoffmann, 1990). However, this is not a concern when alcohol mole fraction $x_A \geq 0.05$, as is the case in this study as well as in industry. Further, for the case of ETBE synthesis over Amberlyst-15, the effectiveness factor has been shown to be around unity at a temperature of 343 K (Sundmacher et al., 1995).

However, diffusion limitations are dependent not only upon temperature, but also upon composition. Thus, to more closely assess the impact of diffusion limitation on the model predictions, the following experiments were conducted. Differential kinetic measurements were conducted in a reaction apparatus similar to that of Zhang and Datta (1995) by varying the WHSV to obtain conversions less than $\sim 5\%$. The net observed rate of reaction could then be calculated simply from the composition difference between the reactor inlet and outlet. Thus, $\eta = r_{obs}/r_{kinetic}$ could be calculated using Eq. 6 for $r_{kinetic}$. Experimental values for the effectiveness factor η were thus obtained for a variety of conditions corresponding to temperature as well as composition values that would exist along the axial direction in a nonisothermal packed-bed reactor for a feed with an ethanol/isobutylene molar ratio of 1.05 and an inlet temperature of 313 K. The results are summarized in Table 1.

These results indicate that the effectiveness factor η does in fact deviate from unity along the length of the reactor. However, this is limited to a very narrow zone in the vicinity of the peak temperature. It is noteworthy that η again approaches unity at the peak temperature, which is not intuitively obvious, since the rate of reaction has become small as equilibrium is approached. To evaluate the impact of such diffusion limitations on the overall model prediction, the effectiveness factor η was included in the rate terms in Eqs. 4 and 5, using numerical values of η extrapolated from the experimental results in Table 1. Model predictions for both cases (that is, $\eta = 1$ and $\eta \neq 1$) are shown in Figure 5. When compared to experimental results, the accuracy of the model is not improved substantially by the inclusion of diffusional limitation terms, except for rounding off of the peak somewhat. This is due to the fact that the region where diffusional limitations are significant is extremely narrow. Thus, it appears that the greatly simplifying assumption of unit effectiveness factor is satisfactory for predictive purposes under the conditions investigated in this study.

Effect of inerts in feed

In industrial synthesis of MTBE or ETBE, the C4 feed consists of substantial amounts of nonreactive species, accounting for up to 50 to 65 wt. % of the feed (Scholz et al., 1990). Thus, to more closely simulate the industrial feed conditions, a feed consisting of 50 wt. % inert (*n*-heptane), and an ethanol/isobutylene molar ratio of 1.05, was used at a total WHSV of 8.7 h^{-1} and an inlet temperature of 318 K. The resulting temperature profile for this case is shown in Figure 6, where it is also compared with the case of no inerts. The presence of the inerts results in a moderation of the peak temperature as well as the shifting of its location farther downstream in the catalyst bed due to a reduction in the reaction rate. Thus the temperature in the presence of inerts

Table 1. Theoretical vs. Experimental Net Reaction Rate along the Axial Direction for a Feed with an Ethanol/Isobutylene Molar Ratio of 1.05 and an Inlet Temperature of 313 K

Distance from Reactor Inlet (cm)	Temp. of Catalyst Bed (K)	Theor. Net Reaction Rate (mol/h·g of Cat)	Exp. Net Reaction Rate (mol/h·g of Cat)	Effectiveness Factor, η
0.0	313	0.044	0.045	1.02
2.5	333	0.278	0.254	0.91
2.7	355	1.409	0.705	0.50
2.75	381	5.733*	1.102	0.19
2.8	389**	0.072	0.069	0.96

*Peak net rate of reaction.
**Peak catalyst-bed temperature.

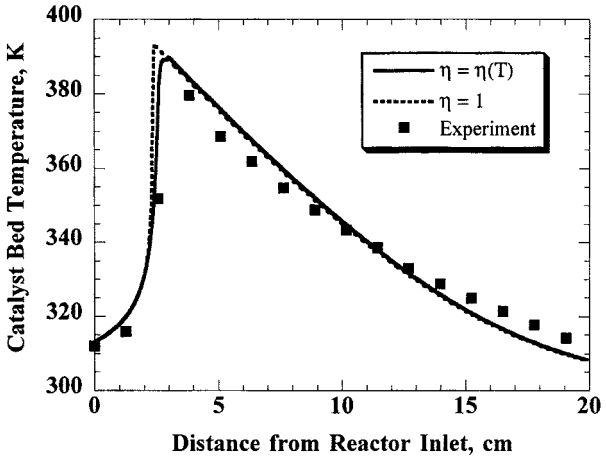

Figure 5. Model comparison between using constant and temperature-dependent effectiveness factor using a feed with no inert.

$\Theta_{EtOH} = 1.05$, WHSV = 4.4 h^{-1}, inlet temperature of 313 K, and $U = 7.0$ J/h·cm^2·K.

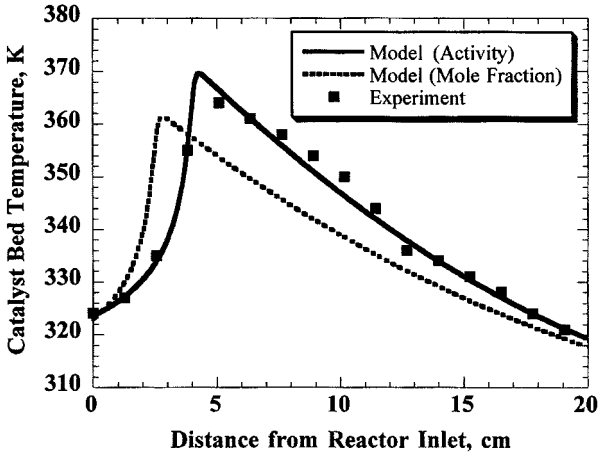

Figure 7. Comparison between using activities vs. mole fractions in rate expression using feed with 50 wt. % inert.

$\Theta_{EtOH} = 1.05$, WHSV = 8.7 h^{-1}, and $U = 7.0$ J/h·cm^2·K.

peaks at around 350 K, whereas in the absence of inerts, the temperature rises to about 392 K. It is seen again that the model describes the experimental data very well in the presence of inerts as well.

While the inert species do not directly appear in the rate expression, they do exert an influence on the rate of reaction by reducing the mole fractions and affecting the activity coefficients of the reactive species. Figure 7 shows the predicted temperature profile when mole fractions replace activities (that is, $\gamma_j = 1$) in the rate expression, Eq. 6, in order to determine the effect of nonideality on the kinetics. It is seen that both the peak temperature and location are drastically affected. Further, the model predictions with $\gamma_j = 1$ are in poor agreement with the experimental results. A much better agreement between experimental and predicted results is obtained when species activities are used in the rate expression.

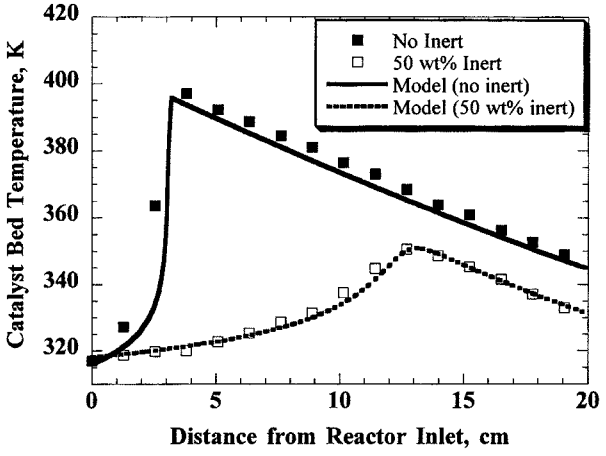

Figure 6. Effect of inerts in reactant stream on the temperature profile with 50 wt. % inert.

$\Theta_{EtOH} = 1.05$, WHSV = 8.7 h^{-1}, inlet temperature of 318 K, and $U = 7.0$ J/h·cm^2·K.

This result further validates the argument that since the reaction mixture is nonideal, activities, rather than concentrations, or mole fractions (Jensen, 1996) are appropriate in the rate expression to provide a proper description of the kinetics of ether synthesis. Of course, this is also consistent with thermodynamics.

Conversion vs. temperature

It is evident from Figure 3 that in a manner similar to the temperature profiles, the conversion profile within the reactor starts at zero conversion at the inlet and rises sharply to the equilibrium conversion. The temperature peak corresponds to the point where equilibrium conversion has been achieved. The conversion thereafter can only be changed by traversing along the equilibrium conversion curve by a decrease in the temperature. This is shown in Figure 8 by directly plotting conversion vs. temperature obtained from the simultaneous solution of Eqs. 4 and 5. Alternatively, X vs. T can be obtained directly by eliminating the axial distance z between Eqs. 4 and 5, or

$$\frac{dX}{dT} = \frac{(-\nu_{iB}) \sum_{j=1}^{n} \Theta_j C_{Pj}^o + \Delta C_{iP}^o X}{(-\Delta H_{iT}^o) + \dfrac{Ua(T_a - T)}{(1-\epsilon_B)\rho_C} \dfrac{1}{r_i}}, \tag{9}$$

and solving this differential equation. The conversion vs. temperature profile shown in Figure 8 corresponds to a 50 wt. % inert feed and an inlet temperature of 323 K. In the kinetic regime, the conversion increases initially *approximately* linearly with temperature until equilibrium conversion of around 75% is achieved, corresponding to the peak temperature of about 370 K. Beyond this point, as the temperature in the reactor drops due to the heat loss, the conversion traverses the equilibrium curve, eventually increasing to 95%. Therefore, in the two-stage reactor scheme commonly utilized in industry, the latter part of the first reactor and the second

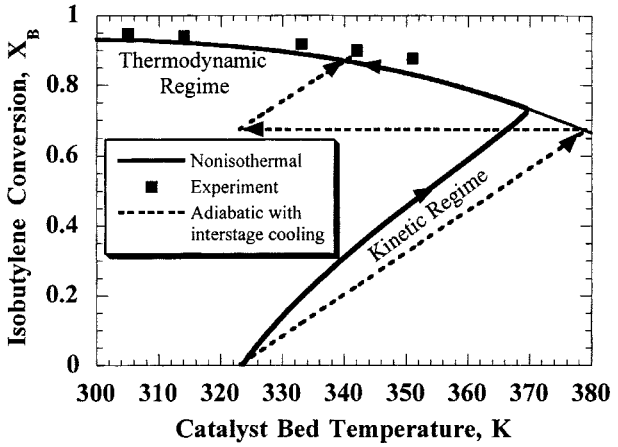

Figure 8. Interrelationship between conversion and temperature for ETBE synthesis in a packed-bed tubular reactor with cooling.

reactor operate in the thermodynamic regime, enhancing the conversion by cooling the reaction mixture. Finally, the nonlinearity of the curve in the kinetic regime is noteworthy, resulting from the temperature dependence of the thermophysical quantities.

Figure 8 also clearly demonstrates the advantage of nonisothermal reactors as compared to adiabatic reactors for exothermic and reversible reactions. The conversion in a truly adiabatic reactor also increases with increasing temperatures in the kinetic regime, but once the conversion intersects with the equilibrium curve, conversion and temperature in the reactor remain constant thereafter. To achieve higher conversions possible with nonisothermal reactors, additional adiabatic reactors with interstage cooling are thus required.

Control of hot spots

As discussed earlier, the temperature spikes within a narrow region of the reactor. These hot spots are a potential problem, since Amberlyst-15 begins to lose its sulfonic acid groups at the higher temperatures, particularly above 393 K. Overheating causes the release of strongly acidic sulfonic and sulfuric acid (Takesono and Fujiwara, 1980), which can also cause corrosion problems downstream. If the temperature is allowed to increase beyond 414 K, the polymeric backbone of the catalyst also begins to decompose. Therefore, adequate heat-removal provisions must be made to minimize thermal catalyst deactivation. For the packed-bed reactor scheme, the heat can be removed by external cooling along the length of the reactor and/or by recirculating part of the effluent stream (Brockwell et al., 1991). The hot spots are also moderated by the presence of diluents in the reactant stream, which aid in lowering the peak temperature in the reactor (Figure 6). From the viewpoint of deactivation, the excess catalyst in the bed (Figure 3), thus, serves as the ''back-log,'' when the front end of the catalyst bed gradually deactivates and the temperature peak concomitantly migrates downstream.

The location and intensity of peak temperature and conversion can also be controlled by the feed temperature. For a given reactor throughput, the inlet feed temperature can play a significant role in the ''ignition'' of the reactor. The effect

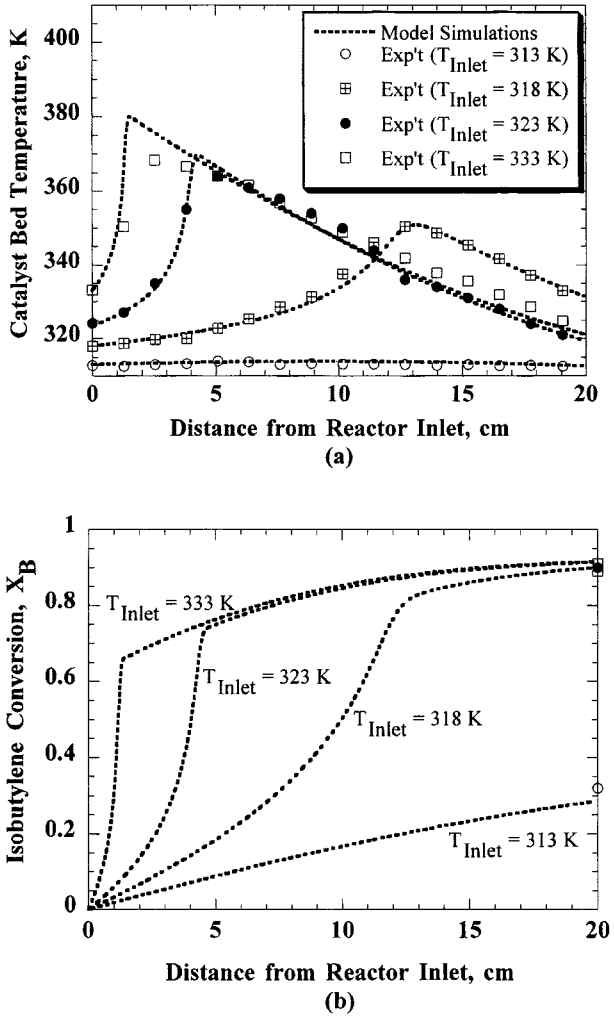

Figure 9. Control of hot spots using inlet feed temperature.

of inlet feed temperature is illustrated in Figure 9 for a feed consisting of 50 wt. % inert (*n*-heptane), an ethanol/isobutylene molar ratio of 1.05, and a WHSV of 8.7 h^{-1}. For temperatures below 313 K, the rate of reaction remains too low throughout the reactor to achieve equilibrium conversions (Figure 9b). For temperatures above and including 318 K, similar equilibrium conversions are achieved, thus achieving the process objective of maximum conversion per unit catalyst. But as the inlet feed temperature increases, so does the peak temperature, and thus consequently the rate of catalyst deactivation. Therefore to maximize conversion and minimize catalyst deactivation an inlet feed temperature of 318 K is indicated under the conditions of this study. Furthermore, at this inlet temperature the catalyst bed is more efficiently used. It is conceivable that as the catalyst ages, the inlet temperature would need to be increased gradually to compensate for the catalyst deactivation.

Conclusions

A one-dimensional model of coupled mass and enthalpy balance is utilized for liquid-phase ETBE synthesis in a non-

isothermal packed-bed reactor that is inherently consistent with reaction thermodynamics, assuming thermochemical properties to be a function of temperature and utilizing a rate expression in terms of activities and incorporating the thermodynamic equilibrium constant. There are few such studies in the literature on nonisothermal packed-bed reactor analysis for liquid-phase reactions. Good agreement was obtained between experimental and predicted results for a variety of conditions, implying that the model is robust and that higher dimensionality and complexity in the model are unnecessary for this system. Further, it is apparent from this study that species activities rather than concentrations, or mole fractions, are appropriate for accurate kinetic description of the nonideal system. In addition, it was shown that although intraparticle diffusion limitations exist within the reactor, the impact to the overall model prediction is minimal due to the narrow region in which the effectiveness factor deviates from unity. Therefore, the use of simpler models that ignore intraparticle diffusion is justified in view of substantial resulting simplicity. The model also simultaneously verifies reaction kinetics as well as thermodynamics of ETBE synthesis by virtue of peak location and subsequent temperature profile, which are highly sensitive to parameters. All the parameters utilized were obtained independently and no fitted parameters were employed.

Notation

a = specific heat-transfer area = $2/R_t$

a_j, b_j, c_j, d_j = coefficients of molar heat capacity expression, Eq. 1

$\Delta a_i = \sum_{j=1}^{n} \nu_{ij} a_j$

$\Delta b_i = \sum_{j=1}^{n} \nu_{ij} b_j$

$\Delta c_i = \sum_{j=1}^{n} \nu_{ij} c_j$

$\Delta d_i = \sum_{j=1}^{n} \nu_{ij} d_j$

a_j = activity of species j, $= \gamma_j x_j$

ΔC_{iP}^{o} = liquid-phase heat capacity difference between products and reactants of reaction i,

$$\Delta C_{iP}^{o} = \sum_{j=1}^{n} \nu_{ij} C_{Pj}^{o}, \text{ J/(mol·K)}$$

$F_j, F_{j_{in}}$ = molar flow rate of species j; inlet molar flow rate of species j, mol/h

ΔG_{fjT}^{o} = standard Gibbs energy of formation of species j in liquid-phase at temperature T, kJ/mol

ΔH_{fjT}^{o} = standard enthalpy of formation of species j in liquid-phase at temperature T, kJ/mol

K_i = thermodynamic equilibrium constant of reaction i

n = total number of chemical species

R = gas constant, 8.3143 J/mol·K

r_i = rate of reaction for reaction i, mol/h·g

W = catalyst mass in reactor, g

x_j = mole fraction of species j, $= F_j \Big/ \sum_{j=1}^{n} F_j$

γ_j = activity coefficient of species j

ν_{ij} = stoichiometric coefficient of species j in reaction i

$\Delta \nu_i$ = change in number of moles of reaction i, $= \sum_{j=1}^{n} \nu_{ij}$

Θ_j = molar feed ratio of species j with respect to isobutylene (B), N_{j0}/N_{A0}

ρ_C = catalyst particle density, g/cm^3

Subscripts

A, B, D = ethanol, isobutylene, ethyl *tert*-butyl ether, respectively

e = at equilibrium

f = of formation

i = of reaction i

j = of species j

T = at temperature T

T^o = at standard temperature

Literature Cited

Aris, R., *Elementary Chemical Reactor Analysis*, Prentice Hall, Englewood Cliffs, NJ (1969).

Brockwell, H. L., P. R. Sarathy, and R. Trotta, "Synthesize Ethers," *Hydrocarbon Process*, 133 (Sept. 1991).

Carberry, J. J., *Chemical and Catalytic Reaction Engineering*, McGraw-Hill, New York, (1976).

Denbigh, K. G., and J. C. R. Turner, *Chemical Reactor Theory*, Cambridge Univ. Press, Cambridge (1984).

Ferreira, R. M. Q., C. A. Costa, and A. Rodrigues, "Heterogeneous Models of Tubular Reactors Packed with Ion-Exchange Resins: Simulation of the MTBE Synthesis," *Ind. Eng. Chem. Res.*, **35**, 3827 (1996).

Froment, G. F., and K. B. Bischoff, *Chemical Reactor Analysis and Design*, 2nd ed., Wiley, New York (1990).

Holland, C. D., and Anthony, *Fundamentals of Chemical Reaction Engineering*, Prentice-Hall, Englewood Cliffs, NJ (1979).

Izquierdo, J. F., F. Cunill, M. Vila, J. Tejero, and M. Iboraa, "Equilibrium Constants for Methyl *tert*-Butyl Ether Liquid Phase Synthesis," *J. Chem. Eng. Data*, **37**, 339 (1992).

Jensen, K. L., and R. Datta, "Ethers from Ethanol: 1. Equilibrium Thermodynamic Analysis of the Liquid-Phase Ethyl *tert*-Butyl Ether Reaction," *Ind. Eng. Chem. Res.*, **34**, 392 (1995).

Jensen, K. L., "Ethyl *tert*-Butyl Ether (ETBE) Synthesis from Ethanol and Isobutylene over Ion-Exchange Resin Catalyst," PhD Thesis, Univ. of Iowa, Ames (1996).

Kitchaiya, P., "Kinetics and Thermodynamics of Tertiary Amyl Ethyl Ether (TAEE) Synthesis on Amberlyst-15," PhD Thesis, Univ. of Iowa, Ames (1995).

Kunin, R., E. Meitzner, J. A. Oline, S. A. Fisher, and N. Frisch, "Characterization of Amberlyst-15," *Ind. Eng. Chem. Prod. Res. Dev.*, **1**, 140 (1962).

Ladisch, M., R. Hendrickson, M. Brewer, and P. Westgate, "Catalyst-Induced Yield Enhancement in a Tubular Reactor," *Ind. Eng. Chem. Res.*, **32**, 1888 (1993).

Lee, H. L., *Heterogeneous Reactor Design*, Butterworth, Boston (1985).

Morse, P. M., "Producers Brace for MTBE Phaseout," *C&E News* (1999).

Rehfinger, A., and U. Hoffmann, "Kinetics of Methyl Tertiary Butyl Ether Liquid Phase Synthesis Catalyzed by Ion Exchange Resin: II. Macropore Diffusion of Methanol as Rate-Controlling Step," *Chem. Eng. Sci.*, **45**, 1619 (1990).

Scholz, B., H. Butzert, J. Neumeister, and F. Nierlich, "Methyl *tert*-Butyl Ether," *Ullman Encyclopedia of Industrial Chemistry*, **A16**, 543, VCM, Wienheim, Germany (1990).

Sundmacher, K., R. Zhang, and U. Hoffmann, "Mass Transfer Effects on Kinetics of Nonideal Liquid Phase Ethyl *tert*-Butyl Ether Formation," *Chem. Eng. Technol.*, **18**, 269 (1995).

Takesono, T., and Y. Fujiwara, "Method for Producing Methyl *tert*-Butyl Ether and Fuel Composition Containing the Same," U.S. Patent No. 4,182,913 (1980).

Tarhan, M. O., *Catalytic Reactor Design*, McGraw-Hill, New York (1983).

Zhang, T. and R. Datta, "Integral Analysis of Methyl *tert*-Butyl Ether Synthesis Kinetics," *Ind. Eng. Chem. Res.*, **34**, 730 (1995).

Manuscript received May 28, 1999, and revision received Oct. 11, 1999.